International Journal on Interactive Design and Manufacturing (IJIDeM) (2020) 14:189–200
https://doi.org/10.1007/s12008-019-00633-z

ORIGINAL PAPER

Development of simulation metamodels to predict the performance and exhaust emission parameters of a spark ignition engine

Erika Zutta[1] · Diego Acosta[1] · Andrés Duque[2] · Adalberto Diaz[1]

Received: 24 February 2019 / Accepted: 23 October 2019 / Published online: 9 November 2019

Abstract
Developing more energy-efficient and environmentally friendly transportation technologies, that can enable to use significantly less petroleum and to reduce regulated emissions while meeting or exceeding drivers' performance expectations, has always been one of the main challenges in automotive technology. Therefore, based on an experimental dataset, metamodels were generated using design of computer experiments and central composite design technique in order to accurately predict carbon monoxide (CO), oxides of nitrogen (NO_x), hydrocarbon (HC) and carbon dioxide (CO_2) emissions, mean effective pressure and exergy destruction due to heat transfer and combustion process. Combustion metamodels was evaluated varying air–fuel ratio, ignition timing [(°CAD) Crank Angle Degrees], compression ratio, and combustion duration (°) on the performance of a Spark Ignition (SI) engine at constant speed of 750 rpm. Because SI gasoline engines always encounter the decreased thermal efficiency and increased toxic emissions at idle (Jurgen in Automotive electronics handbook, McGraw-Hill, New York, 1995). The Akaike information criterion was applied to automatically select the best metamodel for each case.

Keywords Central composite design (CCD) · Response surface methodology (RSM) · Spark-Ignition engine · Exhaust emissions · Engine performance

1 Literature review

Internal combustion (IC) engines have dominated the transportation sector for a century. The high thermal efficiency and high power output-to-volume ratio are two major features that maintain the viability of IC engines as the primary power source in vehicles. But significant variation over crude oil prices, increasing demand of humans for energy production, ever-tightening environmental legislation and depleting petroleum reserves have endangered this viability. Moreover, IC engines are blamed for contributing approximately one fourth of the total greenhouse gases such as Carbon Dioxide (CO_2). IC engines are also contributors of Carbon Monoxide (CO), Nitric Oxide (NO_x), Hydrocarbons (HC) and Particulate Matter (PM) emissions. However, the primary role of IC engines is not expected to be completely replaced by emerging technologies, such as electromotors with high energy density batteries or fuel cells, in the next few decades [2,3]. The mission is to develop more energy-efficient and environmentally friendly transportation technologies that can enable to use significantly less petroleum (Economic Front) and to reduce regulated emissions while meeting or exceeding drivers' performance expectations.

The arrival of computers has created a new branch of scientific and engineering research, namely, numerical simulation. The gas exchange and combustion processes of SI engines are characterized by complex disciplines such as chemical kinetics, fluid dynamics, combustion and thermodynamics. SI engine combustion spans multiple regimes that include flame propagation, mixing-controlled burning, and chemical-kinetics-controlled processes, which may occur simultaneously. The task of modeling SI engines is to completely or partly describe these physical and chemical processes using mathematical models with stable and accu-

✉ Erika Zutta
eszuttag@eafit.edu.co

Diego Acosta
dacostam@eafit.edu.co

Andrés Duque
andres.duquea@udea.edu.co

Adalberto Diaz
gdiaz@eafit.edu.co

[1] Universidad EAFIT, Cra. 49 7sur - 50, Medellín, Colombia

[2] Universidad de Antioquia, Cl. 67 53 - 108, Medellín, Colombia

rate numerical schemes so that the output of the modeling can reveal desirable information about engine cycles.

Early IC modeling studies can be traced back to 1950s when the computing capability of computers only allowed for efficient calculation of simple mathematical formulae. For example, the best known empirical engine model is the Wiebe function [4–6], which is used to predict the burn fraction and burn rate. Progress in engine heat transfer modeling was also made by Woschni [6] who introduced a method for determining the heat transfer coefficient for internal combustion engines and derived an equation containing two convective terms, one of which takes into account the piston motion and the other the convection due to combustion. The model formulae and constants were empirically based on many engine experiments. Such empirical heat transfer models were reviewed by Finol and Robinson [7]. Studies of that age showed that the combination of these empirically based combustion and wall heat release models with well tuned model variables was able to match the pressure traces of engine experimental measurements satisfactorily.

Computational Fluid Dynamics (CFD) in-cylinder engine modeling started in 1970s. However, until the 1980s, engine CFD modeling was not generally applied in engine development due to the computer capacity and general engine CFD code or software was not available. Instead, engine modeling with phenomenological models was the main stream in this period. For instance, coupling of phenomenological quasi-steady spray combustion models and concentration of exhaust NO_x and soot formation models [8–10] largely extended the capability of engine modeling tools compared to zero-dimensional simulations.

In 1985, a group at the Los Alamos National Laboratory developed an opensource code called KIVA [11] which solves the equations of transient multicomponent chemically reactive fluid dynamics, together with those for the dynamics of an evaporating liquid spray. KIVA is a time-marching finite-difference program and provides an open source CFD modeling tool for engine reactive flow simulations, which has significantly stimulated the development of engine physical and chemical models since then. Even though development of physics-based CFD is largely accomplished by being able to conduct detailed simulations of complex geometries, arbitrary numbers of species and chemical reactions and moving boundaries with high-fidelity models describing the relevant physical and chemical interactions. The cost for performing detailed experiments spanning a wide range of operating conditions makes these engine simulations a computationally daunting task. In mentioned cases, researchers must simplify their analyses with the understanding that results may be compromised by lack of fidelity.

Certainly, as the number of actuators associated with these new technologies increases, it introduces an exponential dependency between the time and cost outlays for mapping such complex (high degree of freedom) engines. Furthermore, the increase in the number of the degrees of freedom increases the number of input and output combinations that would have to be tested in order to achieve the calibration objective, making the calibration task virtually impossible. One way of dealing with the increasing complexity in the engine calibration and mapping task is to use the model-based calibration approach which involves the use of statistical methods of Design of Experiments (DoE) [3,12] for reducing the number of engine tests that would be representative of the entire operating space. Actually, from a practical point of view, a reduced set of optimal engine calibrations has to be identified once assigned the required performance targets (minimum fuel consumption, radiated noise and pollutant emissions at part load, maximum power and torque at full load, etc.) and constraints (turbine and catalytic converter inlet temperature, combustion stability, knock avoidance, maximum in-cylinder pressure, etc.).

Therefore, a systematic multivariate analysis could provide a clear and complete knowledge about the combustion characteristics of the engine compared to the one-variable approach in a time study. Then, a statistically valid model is obtained, which by definition contains information on the effects of experimental conditions on the direction and magnitude of the measured response. The required experiments are also performed in a way that maximizes the information that can be extracted from a limited number of experiments [13]. Once a satisfactory model has been determined, it can be used for predicting future observations within the original design range.

Nevertheless, the calibration process may require several months to be experimentally accomplished with an adequate resolution affecting development costs of a new engine [14], [15]. In addition, both physical experiments and high fidelity computer experiments can be time consuming and resource intensive so there is a desire to minimize cost, maximize benefit, and quantify uncertainty [16]. This can be achieved using design of computer experiments (DoCE) and a simplified mathematical model of the system or process being optimized, which advantages include the ability to study a wide range of parametric space and evaluate the long-term effects [17], separated physical and chemical processes, and detailed in-cylinder information, which is normally not available or is inaccessible in experiments. Accordingly, a metamodel is obtained, which is an approximation of the input/output (I/O) function that is defined by the underlying simulation model [18]. Compared to high fidelity computer models and physical experiment data, metamodels enable rapid exploration of a design space and provide information about a system in locations that have not been tested in a physical experiment or computer simulation. The uncertainty of the information in this unexplored design region can be quantified [19]. Furthermore, the proposed approach aims at enhancing the

interaction between designers ideas and technical features of the spark ignition engine, by means of the useful feedback that metamodels can gather through an iterative process of refinement of the concepts and DoCE.

Therefore it is important to emphasize that interactive design is a constructive approach that tends to ensure innovation by improving user-integration in the design process, fostering the development of virtual prototypes, providing new powerful ways for collaborative design activities and supporting decision-making in a huge field of engineering [20–22]. In order to achieve this, it is necessary to use interactive design tools and methods such as simulation, analytical models, numerical analysis, and relevant design software to continuously optimize product performance under safety, energetic, environmental and economic constraints that lead to innovation results.

On the other hand, the automotive industry is going through a fundamental change by moving from a mechanical to a software-intensive industry in which most innovation and competition rely on software engineering competence [15]. And although DoE has been recently used for studying operating region of internal combustion engines [12,14,23–30]. A large body-of-knowledge on internal combustion engines has no systematic analysis of that knowledge and simulation analysts often change only one factor at a time, and use graphical analysis of the resulting input/output (I/O) data [31–38].

Spark timing determination to achieve a desired combustion phasing continues being an empirical process that occurs during the calibration phase of engine development. This process utilizes a large number of stored surfaces and corrections to account for the wide range of operating environments and conditions that a given engine will experience [39]. Consequently, an obstacle to realizing feed-forward physics-based combustion control is the requirement for a reasonably fast and accurate predictive computational model. In this research, a mathematical and numerical model of flow and combustion process for spark ignition engines is employed for the purpose of real-time combustion prediction developed in [40]. The model gives special attention to identification and quantification of irreversibility of combustion process and energy available basing on the isooctane fuel explosion capable. It was developed using the principles of the first and second law of thermodynamic.

Therefore, the innovative contribution of this article can be recognized in the development of a metamodel characterized by a set of factors allowing an accurate reproduction of performance parameters in the whole-engine map. As better explained in the following, the combustion model was evaluated varying air–fuel ratio (AFR), ignition timing, compression ratio, and combustion duration, which are the most important factors to optimize efficiency and emissions, permitting combustion engines to conform to future emission targets and standards [14,17,41–46]. The data collection was conducted at constant speed of 750 rpm because SI gasoline engines always encounter the decreased thermal efficiency and increased toxic emissions at idle [1]. Vehicles have to spend 25% of its total operating time and consume 30% of its total fuel at idle in cities with heavy traffic congestion [47]. Then, improving the engine idle performance is imperative [48,49].

2 Spark ignition engine model

The model used for the development of this work is a kinetic model of the isooctane combustion process that was developed to quantify gas emissions, in which a skeletal mechanism including 32 species and 61 reactions was developed and is able predict satisfactorily ignition timing, burn rate and the emissions of HC, CO_2, CO, NO_x and MEP [40]. The fuel kinetic oxidation model was constructed using a hierarchical approach, which establish sub-mechanisms for fuel molecules at high and lower temperatures. The model was validated with a prediction error less than 5%.

The solution of this model allowed predict greenhouse emissions and analyse system responses to perturbation actions. The model was implemented on Matlab. Input parameters in the software are compression ratio, air–fuel ratio (AFR), ω (angular engine velocity), θ_0 is the angle where the start of combustion occurs (ignition timing), L/R engine relation, properties of the fuel and ambient pressure and temperature (Fig. 1). It was deployed as a deterministic computer simulator, so repeated runs with the same input values will always produce the same response value. For more information, refer to the article [40].

3 Experimental set-up

3.1 Two-level full factorial design

The effects and statistical significance of a larger group of experimental variables can be determined through factorial designs, which enable choosing the relevant variables or conditions for the next set of experiments. Experimental designs are constructed in a way that eliminates or minimizes correlations between the chosen variables [50]. This allows independent estimation of variable effects and their potential interactions.

Therefore, a unreplicated 2^4 complete factorial was conducted by varying air–fuel ratio (AFR), ignition timing [(°CAD) Crank Angle Degrees], compression ratio, and combustion duration (°) on the performance of a spark ignition engine at constant speed of 750 rpm with engine specifications given in Table 1.

The ranges of the input parameters were selected based on the permissible limits within which the modifications

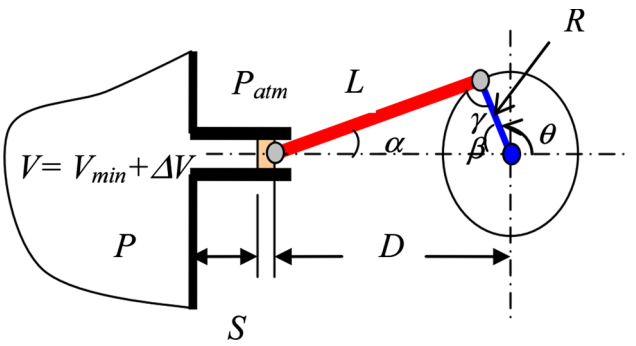

Fig. 1 Scheme of the rod-crank-slipper system proposed for the combustion cylinder rate volume [40]

Table 1 Technical data Renault Twingo (C06) 1.2

Characteristic	Value
Manufacturer	Renault
Series	Twingo
Model	(C06) 1.2
Type of fuel	Petrol
Type of fuel system	Multi-point fuel injection (MPFI)
Engine location	Transverse, front
Engine displacement	1149 cc (cubic centimeters)
Valve mechanism type	Overhead camshaft (OHC)
Type of aspiration	Naturally aspirated
Compression ratio	9.60:1
Arrangement of the cylinders	inline/straight engine
Number of cylinders	4 (four)
Valves per cylinder	2 (two)
Bore (the diameter of a cylinder)	69.00 mm (millimeters)
Stroke (the length of a piston stroke)	76.80 mm (millimeters)

can be made with the existing engine set up. The performance parameters evaluated were carbon monoxide (CO (mg/m^3)), oxides of nitrogen (NO (mg/m^3)), hydrocarbon (HC (mg/m^3)) and carbon dioxide (CO_2 (mg/m^3)) emissions, mean effective pressure [MEP—(Pa)] and exergy destruction due to heat transfer (J) and combustion process (J).

The standard layout for a 2-level design uses $+1$ and -1 notation, called coding the data, to denote the "high level" and the "low level" respectively, for each factor. After factor settings are coded, center points have the value "0". The following algorithm for unreplicated 2^4 factorial design was proposed [18]:

1. Linear Regression. General representation for linear regression models with four inputs and a single output was applied.

$$\begin{aligned}\hat{y} = {} & \beta_0 + \beta_1 x_1 + \beta_2 x_2 + \beta_3 x_3 + \beta_4 x_4 + \beta_5 x_1 x_2 \\ & + \beta_6 x_1 x_3 + \beta_7 x_1 x_4 + \beta_8 x_2 x_3 + \beta_9 x_2 x_4 \\ & + \beta_{10} x_3 x_4 + \beta_{11} x_1 x_2 x_3 + \beta_{12} x_1 x_2 x_4 \\ & + \beta_{13} x_1 x_3 x_4 + \beta_{14} x_2 x_3 x_4 + \beta_{15} x_1 x_2 x_3 x_4 + \varepsilon \quad (1)\end{aligned}$$

where $\hat{y}$ denotes the dependent variable; x_i denotes the value of independent variable; β_j denotes the regression parameters; and ε denotes the residual.

2. Outliers, typos and obvious problems were examined by constructing many graphs to get the big picture. Identifying important factors by the aid of:
   - 2.1 Daniel Plot: Can be used to estimate the error standard deviation and to make judgments about the reality of the observed effects [51].
   - 2.2 Lenth Plot: Effective alternative method for formal analysis of unreplicated factorials. It is based on a simple formula for the standard error of the contrast estimates. The usual t procedures can be used to interpret the results. Thus both the size and "significance" of the contrasts by looking at just one graph can be assessed [52].
   - 2.3 Interaction plots.
3. Tentative meta-models were selected from the data and was simplify using the information gotten in step 2. and parameter p value significance information.
4. Given a set of candidate models for the data, the preferred model is the one with the minimum Akaike information criterion (AIC) value [53].
5. The equation Eq. 2 was used to determine the presence of curvature according to Sect. 3.2 in order to fit a quadratic model that includes square terms to model the curvature and analyse the results.

$$|(\overline{y} - y_c)| \leq 3SE \quad (2)$$

where $\overline{y}$ is the value of the intercept of the first-order model and y_c is the response variable in the central test. When curvature in the design space was found, a quadratic model was proposed to model the curvature and to analyse the results (see Sect. 3.2). In the absence of curvature, factor configuration was used to optimize the response.

3.2 Central composite design

The experiments were organized according to a central composite design (CCD) with four variables and one replicated center-point experiment. The design included five levels for each variable $(-2, -1, 0, 1, 2)$ and can be used for quantifying linear, interaction and higher-order model terms. After having executed the 2^4 full factorial, augmentation of that design to a central composite design (CCC) was accom-

plished by adding an additional set (block) of star and centerpoint run. If the factorial experiment indicated (via the t test) curvature, this composite augmentation was the best follow-up option. Subsequently a response surface methodology was conducted (see Sect. 3.3).

3.3 Response surface method (RSM)

The response surface method (RSM) as a collection of statistical and mathematical methods, is well known as a useful method for analyzing engineering problems based on both the modeling and the optimization [13]. Further, RSM generally uses the Design of Experiments (DoE) to obtain data using a structured test plan and then, in general, uses regression models to study the relationship between the independent and response variables. These models drive the DoE towards greater data acquisition or final motor calibrations.

The simplest model which can be used in RSM is based on a linear function presents the following Eq. 3

$$\hat{y} = \beta_0 + \sum_{i}^{k} \beta_i x_i + \varepsilon \tag{3}$$

If this model presents any curvature, a second-order model must be used as the following Eq. 4

$$\hat{y} = \beta_0 + \sum_{i}^{k} \beta_i x_i + \sum_{i<k}^{k} \beta_{ij} x_i x_j + \varepsilon \tag{4}$$

For the present study, quadratic model is suitable to determine a critical function point (maximum, minimum), using Eq. 5

$$\hat{y} = \beta_0 + \sum_{i}^{k} \beta_i x_i + \sum_{i}^{k} \beta_{ii} x_i^2 + \sum_{i<k}^{k} \beta_{ij} x_i x_j + \varepsilon \tag{5}$$

where k is the number of variables (for this case k = 4), x_i, x_j and x_i^2 represent variables. β_0, β_i, β_{ii} and β_{ij} are the constant term, the coefficients of the linear terms x_i, the coefficients of the quadratic terms x_i^2 and the coefficients of the interaction terms $x_i x_j$ respectively. ε is the residual associated to the experiments. The steps for fitting a response surface (second-order or quadratic) model were as follows:

1. Full second order model was fitted.
2. Stepwise regression was used to identify important variables.
3. When selecting variables for inclusion in the model, the hierarchy principle was followed and all main effects were kept that are part of significant higher-order terms or interactions, even if the main effect p value was larger than desired. A model was selected according to the Akaike information criterion.
4. Diagnostic residual plots such as histograms, box plots, normal plots were generated for the model selected. The fitted model plot, interaction plots, and ANOVA statistics and Lack-of-fit test were examined. All these plots and statistics to determine whether the model fit was satisfactory were used.
5. Breusch–Pagan test,was used to test for heteroskedasticity in the regression model (using the function ncvTest of car package provided to R). It tests whether the variance of the errors from a regression is dependent on the values of the independent variables. In that case, heteroskedasticity is present . If heteroskedasticity was present, a change of response variable was made according to the pattern of the residuals and the process was repeated from step 1. A heteroskedasticity check is required to accompany before stepping to any further analysis. Since, ignoring the presence of heteroskedasticity may result in inaccurate inferences, for instance, inefficient or even inconsistent estimates [54].

All the above steps for each response variables were repeated. Rsm package of R was used to generate central-composite designs and response-surface.

4 Results and discussion

The results obtained from the full factorial can be seen in the Table 2, runs 1–16 and centerpoint run 17. The mentioned matrix describes an experiment in which 16 runs were conducted with each factor set to high or low during a run. All the columns of the two-level full factorial design are orthogonal. That is, the dot product for any pair of columns is zero.

In addition, the results obtained from CCD can be seen in the Table 2, runs 18 to 25 and centerpoint run 17. R software was used to data analysis, particularly, BsMD package.

A multiple regression analysis was carried out to obtain the coefficient and the equations, which can be used to predict the responses. Using the statistically significant model, the correlation between the process parameters and the several responses were obtained.

The Daniel and Lenth graphs for each of the output variables can be found in Figs. 2 and 3. When Lenth and Daniel's plots showed different results, the final model was chosen by the Akaike criterion.

This study began with first order response surfaces (see Table 3) and progressed to second order (see Table 4). The second order polynomial equation based on the coded values that was obtained using multiple regression analysis of the data is presented in the Table 5.

Table 2 Unreplicated 2^4 factorial design

Run	X_1		X_2		X_3		X_4		Y_1	Y_2	Y_3	Y_4	Y_5	Y_6	Y_7
1	− 1	(13.5)	− 1	(− 20)	− 1	(8)	− 1	(40)	5534.957	3.9048	3512.057	1572.759	3377618	300.714	325.314
2	1	(16.5)	− 1	(− 20)	− 1	(8)	− 1	(40)	5368.395	6.6632	5749.141	2153.086	3347858	299.031	322.267
3	− 1	(13.5)	1	(− 10)	− 1	(8)	− 1	(40)	3733.130	5.8293	3989.455	1491.313	3212355	278.645	337.337
4	1	(16.5)	1	(− 10)	− 1	(8)	− 1	(40)	3086.189	6.6398	6324.982	2013.246	3189110	276.951	334.249
5	− 1	(13.5)	− 1	(− 20)	1	(10)	− 1	(40)	7100.830	4.6009	4531.015	1995.261	3555120	312.443	323.419
6	1	(16.5)	− 1	(− 20)	1	(10)	− 1	(40)	6809.284	7.5385	7498.974	2756.043	3522614	310.698	320.384
7	− 1	(13.5)	1	(− 10)	1	(10)	− 1	(40)	4430.101	6.3817	5719.612	1999.977	3331796	286.215	336.718
8	1	(16.5)	1	(− 10)	1	(10)	− 1	(40)	3558.032	7.0436	8723.307	2653.764	3307286	284.475	333.661
9	− 1	(13.5)	− 1	(− 20)	− 1	(8)	1	(60)	3329.905	1.9431	1890.305	1010.870	4105160	458.503	331.356
10	1	(16.5)	− 1	(− 20)	− 1	(8)	1	(60)	3321.757	2.2100	3092.099	1339.366	4041521	456.001	328.315
11	− 1	(13.5)	1	(− 10)	− 1	(8)	1	(60)	2567.715	3.5185	1784.142	864.7692	3768630	414.785	345.389
12	1	(16.5)	1	(− 10)	− 1	(8)	1	(60)	2382.205	2.8026	2980.009	1170.984	3724302	412.237	342.330
13	− 1	(13.5)	− 1	(− 20)	1	(10)	1	(60)	4281.295	2.2055	2415.054	1263.972	4333074	469.656	331.843
14	1	(16.5)	− 1	(− 20)	1	(10)	1	(60)	4264.968	2.7785	3964.289	1683.406	4266100	467.100	328.819
15	− 1	(13.5)	1	(− 10)	1	(10)	1	(60)	3195.010	5.1162	2493.532	1137.511	3921135	419.622	346.724
16	1	(16.5)	1	(− 10)	1	(10)	1	(60)	2828.084	3.7168	4194.572	1552.923	3875910	417.046	343.659
17	0	(15)	0	(− 15)	0	(9)	0	(50)	4197.245	3.2428	3754.827	1544.335	3693290	366.651	332.535
18	− 2	(12)	0	(− 15)	0	(9)	0	(50)	4323.557	2.581	1920.517	1042.990	3743380.5	369.267	336.2918
19	2	(18)	0	(− 15)	0	(9)	0	(50)	3857.423	4.281	5697.848	2017.497	3660284.8	364.891	330.0171
20	0	(15)	− 2	(− 25)	0	(9)	0	(50)	5607.745	2.506	4142.757	1867.179	3999666.0	401.608	315.2130
21	0	(15)	2	(− 5)	0	(9)	0	(50)	2391.337	3.440	4465.853	1514.195	3444770.6	332.372	343.3536
22	0	(15)	0	(− 15)	− 2	(7)	0	(50)	3208.857	2.565	2698.174	1157.458	3521033.3	358.531	332.5697
23	0	(15)	0	(− 15)	2	(11)	0	(50)	5134.788	3.706	4854.244	1939.293	3858276.5	376.498	332.4496
24	0	(15)	0	(− 15)	0	(9)	− 2	(30)	5037.071	13.26	9272.897	2880.489	2844285.2	218.988	330.2855
25	0	(15)	0	(− 15)	0	(9)	2	(70)	2660.113	1.206	2085.290	1004.502	4253304.1	509.900	346.2098

X_1: Air–fuel ratio
X_2: Ignition timing (°CAD)
X_3: Compression ratio
X_4: Combustion duration (°)
Y_1: Carbon dioxide emissions (mg/m^3)
Y_2: Carbon monoxide emissions (mg/m^3)
Y_3: Hydrocarbons emissions (mg/m^3)
Y_4: Oxides of nitrogen emissions (mg/m^3)
Y_5: Mean effective pressure (Pa)
Y_6: Exergy destruction due to heat transfer/(J)
Y_7: Exergy destruction due to combustion process/(J)

4.1 Carbon dioxide emission

The effect of the linear factors, X_2: Ignition Timing, X_3: Compression Ratio, X_4: Combustion Duration were found to be highly significant on the CO_2 exhaust emission. Similarly, the interactive effect of X_2X_4, which is depicted in Daniel and Lenth graphs, Fig. 2a, b respectively. In addition, as can observed in Table 3, increasing ignition timing and combustion duration, CO_2 emission decreases. A positive sign of the coefficient means a synergistic effect, while a negative sign represents an antagonistic effect. Although the curvature test was negative, the fitted second-order polynomial enables the estimation of the optimum. Full second order polynomial equation based on the coded values was obtained and is presented in Table 4. Final model was selected according to the Akaike information criterion and it approved the Breusch–Pagan test as a homoscedastic structure, see Table 5. In this case, the R^2 obtained was 0.9085.

4.2 Carbon monoxide emission

Although all factors turned out to be significant according to Daniel's graph (see Fig. 2c). The factor with the greatest influence on the generation of CO is X_4: Combustion Duration, whose significance is highlighted in Lenth's graph (see Fig. 2d). Correspondingly, the interactions of X_1X_2 and

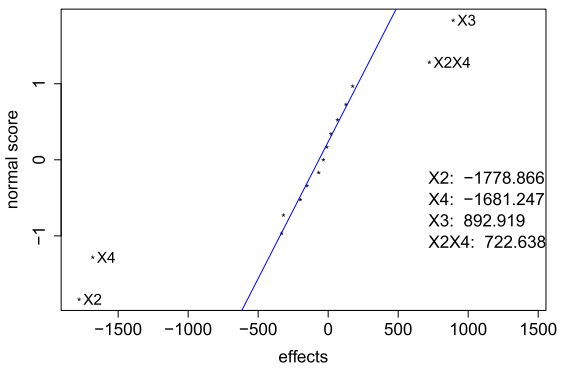

(a) Carbon Dioxide (CO_2) Emissions Daniel Plot

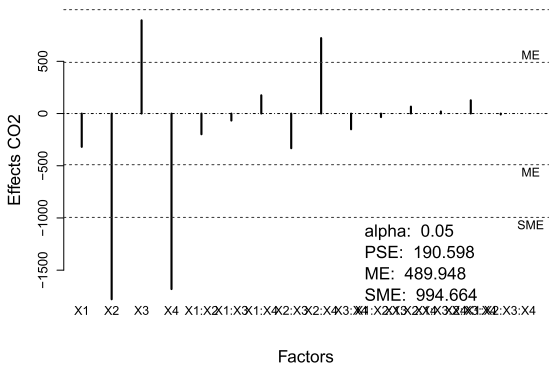

(b) Carbon Dioxide (CO_2) Emissions Lenth Plot

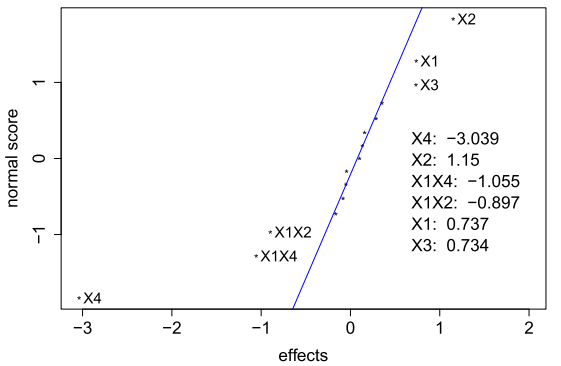

(c) Carbon Monoxide (CO) Emissions Daniel Plot

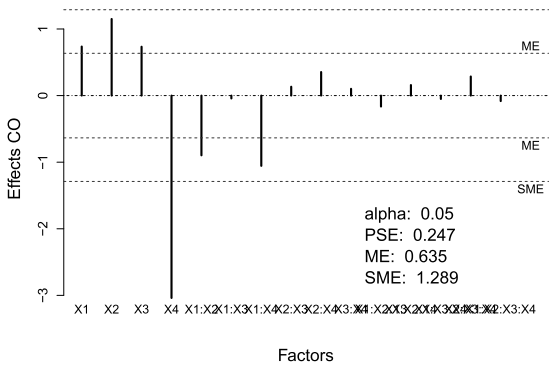

(d) Carbon Monoxide (CO) Emissions Lenth Plot

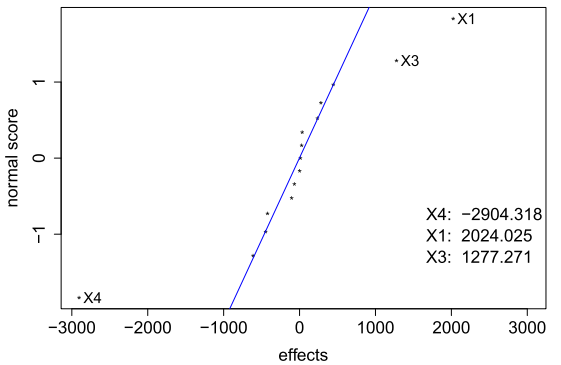

(e) Hydrocarbons (HC) Emissions Daniel Plot

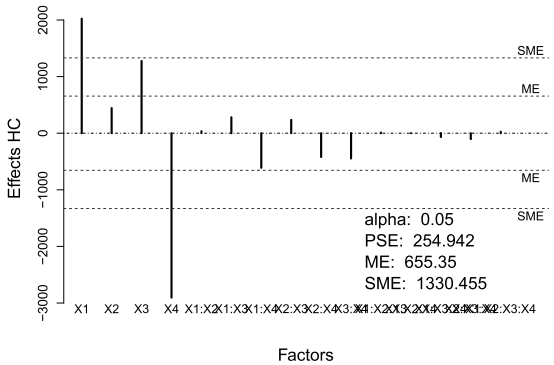

(f) Hydrocarbons (HC) Emissions Lenth Plot

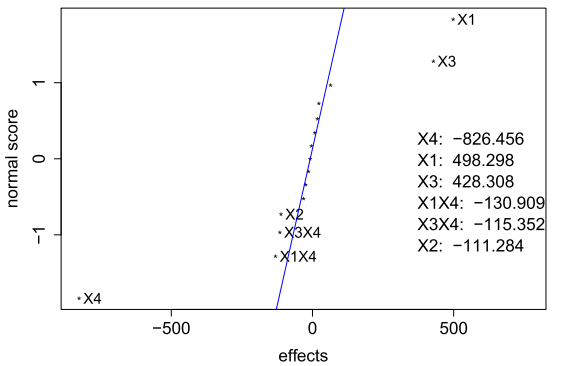

(g) Oxides of Nitrogen (NO_x) Emissions Daniel Plot

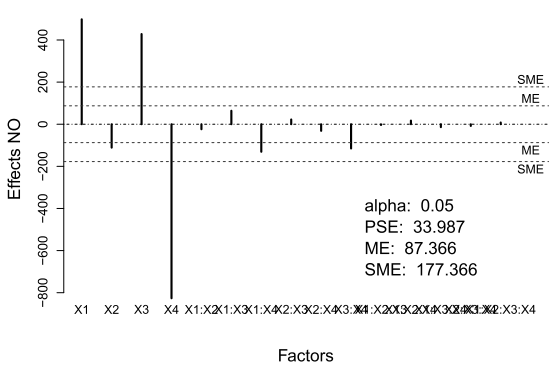

(h) Oxides of Nitrogen (NO_x) Emissions Lenth Plot

Fig. 2 Exhaust gases response variables

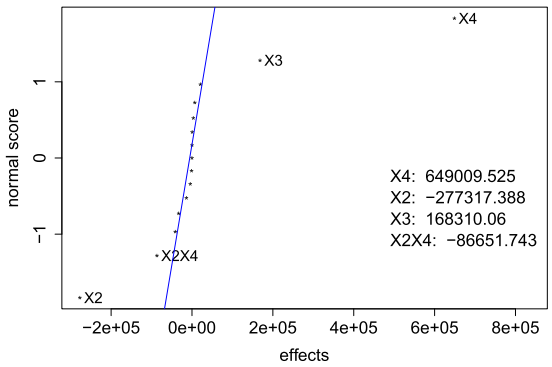

(a) Mean Effective Pressure (MEP) Daniel plot

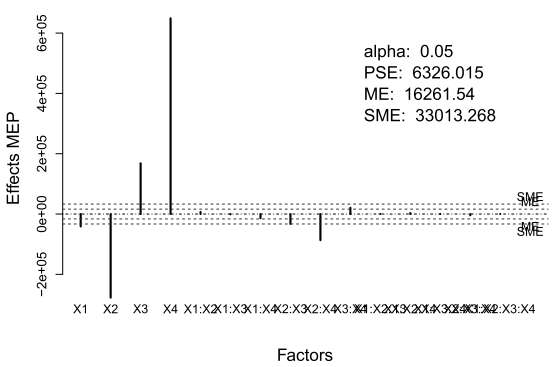

(b) Mean Effective Pressure (MEP) Lenth plot

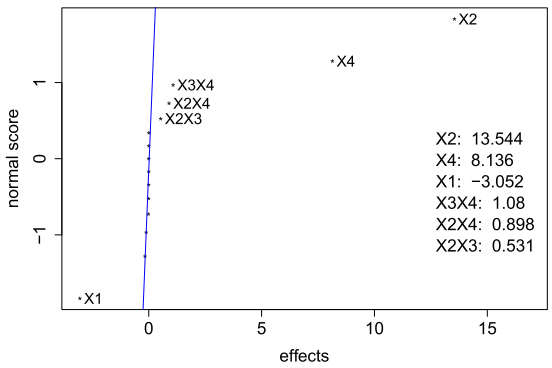

(c) Exergy Destruction due to Combustion Process Daniel plot

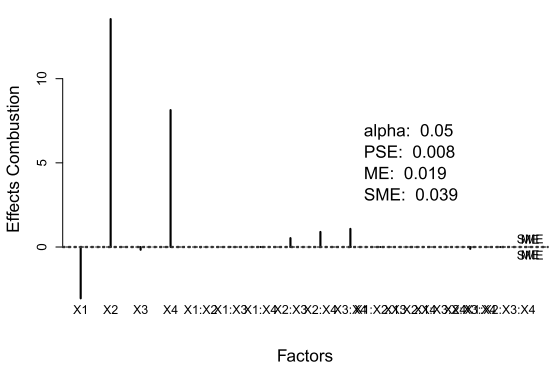

(d) Exergy Destruction due to Combustion Process Lenth plot

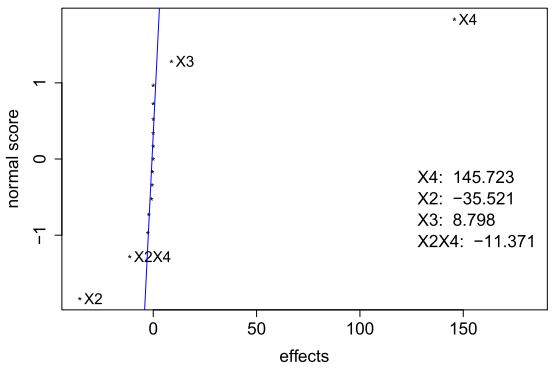

(e) Exergy Destruction due to Heat Transfer Daniel plot

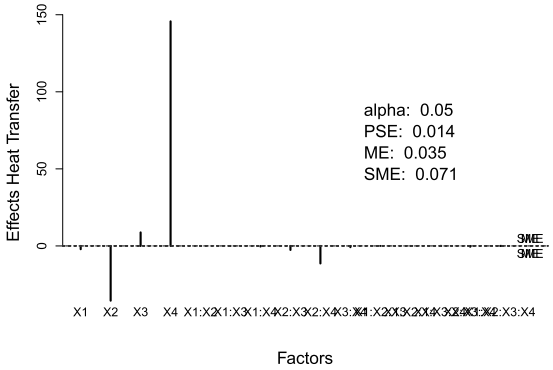

(f) Exergy Destruction due to Heat Transfer Lenth plot

Fig. 3 Engine performance response variables

X_1X_4 were also significant. As can be found in Table 3, increasing combustion duration, CO emission considerably decreases. The curvature test was negative. But, full second order polynomial equation is introduced in Table 4. Final model was selected according to the Akaike information criterion and it approved the Breusch–Pagan test as a homoscedastic structure, see Table 5. Finally, the R^2 obtained was 0.9085.

4.3 Hydrocarbons emission

According to Daniel's and Lenth's graphs, Fig. 2e, f respectively, the significant factors are X_1: air–fuel ratio, X_3: compression ratio, X_4: combustion duration. First order metamodel can be found in Table 3, from which it is concluded that increasing X_1 and X_3, HC emission raises. Otherwise, increasing the value of X_4, the generation of HC drops.

Table 3 Summary linear regression models

Output variable	Model	Multiple R-squared (R^2)
Y_7	$\widehat{Y_7} \sim 333.237 - 1.526X_1 + 6.772X_2 - 0.083X_3 + 4.068X_4 + 0.265X_2X_3 + 0.449X_2X_4 + 0.539X_3X_4$	0.9999
Y_6	$\widehat{Y_6} \sim 366.508 - 17.760631X_2 + 4.399X_3 + 72.861X_4 - 5.685X_2X_4$	0.9994
Y_5	$\widehat{Y_5} \sim 3679974.17 - 20636.73X_1 - 138658.69X_2 + 84155.03X_3 + 324504.76X_4 - 43325.87X_2X_4 - 16438.85X_2X_3$	0.9986
Y_4	$\widehat{Y_4} \sim 1666.203 + 249.149X_1 - 55.642X_2 + 214.154X_3 - 413.2281X_4 - 65.454X_1X_4 - 57.676X_3X_4$	0.9941
Y_2	$\widehat{Y_2} \sim 4.556+0.368X_1+0.575X_2+0.367X_3-1.519X_4-0.448X_1X_2-0.528X_1X_4$	0.9784
Y_1	$\widehat{Y_1} \sim 4111.991 - 889.432X_2 + 446.459X_3 - 840.624X_4 + 361.319X_2X_4$	0.9565
Y_3	$\widehat{Y_3} \sim 4303.910 + 1012.013X_1 + 638.635X_3 - 1452.159X_4$	0.9277

The curvature test was positive. Therefore, adjusting a superior order model is mandatory. Additionally, the presence of heteroscedasticity was a major concern in the application of regression analysis during adjustment of the second order model (see Table 4). Fortunately this problem could be figured out using Poisson transformation, according to the pattern of the residuals. Finally, the model obtained has R^2 equals to 0.99397 and it delivers the square root of the amount of HC generated.

4.4 Oxides of nitrogen emission

According to Lenth's graph, the significant factors are X_1, X_3 and X_4. And from Daniel graph, the factor X_2 and the interactions X_3X_4 and X_1X_4 were added. According to the obtained results, the factors that increase the NO emission are X_1 and X_3. And the factors that could reduce the generation of NO_X are X_2, X_4. The first order model obtained is in Table 3, whose curvature test was positive.

The full second order model can be observed in the Table 4, which has R^2 of 0.9964. Final model was selected according to the Akaike information criterion and it approved the Breusch–Pagan test as a homoscedastic structure, see Table 5. In this case, the R^2 reached was 0.99601.

4.5 Mean effective pressure

According to Daniel's graph (Fig. 3a), the significant factors are X_2, X_3, X_4 and the interaction X_2X_4. In order to obtain the most appropriate first order model, the effects of the factor X_1 and the interaction of X_2X_3 were added, according to the information given by Lenth's graph (Fig. 3b). The factor with the greatest influence on the output of the metamodel is X_4. This influence is positive (see Table 3).

The curvature test was negative. The full second order model is illustrated in Table 4, and R^2 reached was 0.9984. Additionally, the presence of heteroscedasticity was detected by fitting the second order model. Fortunately this problem could be figured out removing the outlier that corresponds to the combination $X_1 = 0$, $X_2 = 0$, $X_3 = 0$ and $X_4 = -2$, which delivered a value of 2844285.2 Pa as mean effective pressure, see run 24 in Table 2. Finally, the model obtained has R^2 equals to 0.9998 and it is described in the Table 5.

4.6 Exergy destruction due to heat transfer

The effect of the linear factors, X_1, X_3 and X_4 were found to be highly significant on exergy destruction due to heat transfer, which is depicted in Daniel's and Lenth's graphs, Fig. 3e, f respectively. In addition, as can be seen in Table 3, the increment exergy destruction due to heat transfer is a consequence of the increment in the factors X_3 and X_4 or the reduction of the factor X_2.

Although the curvature test was negative, the fitted second-order polynomial enables the estimation of the optimum. Full second order polynomial equation was obtained and is presented in Table 4. Final model was selected according to the Akaike information criterion and it approved the Breusch–Pagan test as a homoscedastic structure, see Table 5. In this case, R^2 obtained was 0.99994.

4.7 Exergy destruction due to combustion process

According to Daniel's and Lenth's graph (see Fig. 3d and 3c), the significant factors are X_1, X_2, X_4 and the significant interactions are X_3X_4, X_2X_4 and X_2X_3. When selecting variables for inclusion in the model, the hierarchy principle was followed and all main effects that are part of significant higher-order terms or interactions were kept, even if p value of X_3 was larger than desired.

The curvature test was positive. The full second order model can be observed in the Table 4, which has R^2 of 0.9996. Final model was selected according to the Akaike information criterion and it approved the Breusch–Pagan test as a

Table 4 Summary full second order models

Output variable	Model	Multiple R-squared (R^2)
Y_6	$\widehat{Y_6} \sim 366.652 - 1.077X_1 - 17.61X_2 + 4.4301X_3 + 72.817X_4 - 0.004X_1X_2 - 0.012X_1X_3 - 0.207X_1X_4 - 1.307X_2X_3 - 5.685X_2X_4 - 0.412X_3X_4 + 0.104X_1^2 + 0.085X_2^2 + 0.216X_3^2 - 0.551X_4^2$	0.9999
Y_7	$\widehat{Y_7} \sim 332.536 - 1.542X_1 + 6.859X_2 - 0.0654X_3 + 4.039X_4 - 0.0076X_1X_2 + 0.003X_1X_3 + 0.002X_1X_4 + 0.265X_2X_3 + 0.449X_2X_4 + 0.539X_3X_4 + 0.143X_1^2 - 0.823X_2^2 - 0.016X_3^2 + 1.418X_4^2$	0.9996
Y_5	$\widehat{Y_5} \sim 3693290.379 - 21195.565X_1 - 138680.42X_2 + 84206.95X_3 + 333754.748X_4 + 3473.088X_1X_2 - 515.232X_1X_3 - 6884.131X_1X_4 - 16438.847X_2X_3 - 43325.871X_2X_4 + 10420.72X_3X_4 + 3885.704X_1^2 + 9751.763X_2^2 + 1610.918X_3^2 - 33604.138X_4^2$	0.9984
Y_4	$\widehat{Y_4} \sim 1544.335 + 247.333X_1 - 66.51X_2 + 207.9222949X_3 - 431.817X_4 - 11.98X_1X_2 + 32.028X_1X_3 - 65.454X_1X_4 + 11.329X_2X_3 - 15.786X_2X_4 - 57.676X_3X_4 - 5.45X_1^2 + 34.624X_2^2 - 0.954X_3^2 + 97.576X_4^2$	0.9964
Y_3	$\widehat{Y_3} \sim 3754.827 + 987.8X_1 + 175.119X_2 + 605.429X_3 - 1567.073X_4 + 17.503X_1X_2 + 140.728X_1X_3 + -306.02X_1X_4 + 117.919X_2X_3 + -210.978X_2X_4 - 223.523X_3X_4 - 3.19X_1^2 + 123.067X_2^2 - 8.956X_3^2 + 466.765X_4^2$	0.9911
Y_1	$\widehat{Y_1} \sim 4197.246 - 145.199X_1 - 860.989X_2 + 458.134X_3 - 758.495X_4 - 99.304X_1X_2 - 33.738X_1X_3 + 87.513X_1X_4 - 166.211X_2X_3 + 361.319X_2X_4 - 75.487X_3X_4 - 12.546X_1^2 - 35.378X_2^2 + 7.691X_3^2 - 73.116X_4^2$	0.9875
Y_2	$\widehat{Y_2} \sim 3.243 + 0.378X_1 + 0.461X_2 + 0.339X_3 - 2.017X_4 - 0.448X_1X_2 - 0.0216X_1X_3 - 0.527X_1X_4 + 0.066X_2X_3 + 0.177X_2X_4 + 0.051X_3X_4 + 0.097X_1^2 - 0.005X_2^2 + 0.036X_3^2 + 1.06X_4^2$	0.9143

Table 5 Summary simplified and transformed second order model

Output variable	Model	Multiple R-squared (R^2)
Y_6	$\widehat{Y_6} \sim 367.036 - 1.074X_1 - 17.61X_2 + 4.43X_3 + 72.817X_4 - 1.307X_2X_3 - 5.685X_2X_4 - 0.608X_4^2$	0.99994
Y_5	$\widehat{Y_5} \sim 3695228.782 - 20223.82X_1 - 138680.42X_2 + 84206.95X_3 + 324371.757X_4 - 6884.132X_1X_4 - 43325.87X_2X_4 - 16438.85X_2X_3 + 10420.72X_3X_4 + 6880.395X_2^2 - 22401.019X_4^2$	0.9998
Y_7	$\widehat{Y_7} \sim 332.514 - 1.541X_1 + 6.859X_2 - 0.065X_3 + 4.039X_4 + 0.265X_2X_3 + 0.449X_2X_4 + 0.539X_3X_4 + 0.143X_1^2 - 0.823X_2^2 + 1.421X_4^2$	0.99969
Y_4	$\widehat{Y_4} \sim 1536.279 + 246.351X_1 - 66.510X_2 + 207.922X_3 - 431.817X_4 - 11.98X_1X_2 + 32.027X_1X_3 - 65.454X_1X_4 - 15.786X_2X_4 - 57.676X_3X_4 + 36.044X_2^2 + 98.996X_4^2$	0.99601
Y_1	$\widehat{Y_1} \sim 4158.788 - 146.037X_1 - 860.989X_2 + 458.138X_3 - 758.495X_4 - 99.303X_1X_2 + 87.512X_1X_4 - 166.21X_2X_3 + 361.318X_2X_4 - 75.487X_3X_4 - 67.297X_4^2$	0.98617
Y_2	$\widehat{Y_2} \sim 3.376 + 0.396X_1 + 0.461X_2 + 0.339X_3 - 2.017X_4 - 0.448X_1X_2 - 0.527X_1X_4 + 1.06X_4^2$	0.90853
Y_3	$\sqrt{\widehat{Y_3}} \sim 60.552 + 7.725X_1 + 1.166X_2 + 4.646X_3 - 11.635X_4 + 0.518X_1X_3 - 1.053X_1X_4 - 1.399X_2X_4 - 0.891X_3X_4 + 1.147X_2^2 + 2.493X_4^2$	0.99397

homoscedastic structure, see Table 5. In this case, the R^2 reached was 0.99969.

5 Conclusions and future work

The Design of experiments was useful tool to quantify the effect of different factors on exhaust emissions and performance parameters by constructing metamodels. This design of experiment considerably reduced the time required by minimizing the number of experiments to be performed and presented a metamodel for each response. From the outcome of this research, the following conclusions are drawn:

- The function of exergy destruction due to combustion process presented the best performance with R^2 values around 0.9999. In Table 5 is described information of the other metamodels. Most of these have a R^2 higher than 0.98.
- About 97% of the residuals were within the $\pm 3\%$ range, which is a very good accuracy index. The metamodels were also able to provide the estimation of standard deviations for each individual prediction and almost all experimental values agreed with the 95% confidence interval for their corresponding predictions.
- When many design aspects should be understood by the design team, it is necessary to apply interactive approaches in order to evaluate the effect of different factors on exhaust emissions and performance parameters, allowing the designer to characterize the relationship among the functional requirements and the corresponding design parameters. Furthermore, analysing the performance of a spark ignition engine in a simulation in several operational conditions helps the designer to refine the knowledge of the behaviour under virtual environment that simulates the real conditions in the real time, by modifying certain parameters and by controlling the calculation flows.
- One of the most important contributions of this research lies in the development of a new approach, whose methodology is practical, interactive and delivers more accurate decision support to perform an engine performance analysis and emission parameters comparison. This technique can be utilized in any engine type.

In summary, this work outlined an interactive approach to assess a current design (controllable independents) in its current environment (uncontrollable independents). Because, metamodeling is the enabling link between simulation, DoE and statistical analysis. Wider use of appropriate metamodeling in all stages of the design process will drive efficiency in experiment and result in higher performing products. Nevertheless, the metamodels proposed herein are not universally applicable as the results are bound to be subject to changes in other parameters such as engine operating conditions, which were not considered.

References

1. Jurgen, R.K.: Automotive Electronics Handbook. McGraw-Hill, New York (1995)
2. Shi, Y., Ge, H.-W., Reitz, R.D.: Computational Optimization of Internal Combustion Engines. Springer, New York (2011)
3. Broekaert, S.: A Study of the Heat Transfer in Low Temperature Combustion Engines. PhD thesis, Ghent University (2018)
4. II Vibe. Semi-empirical expression for combustion rate in engines. In: Proceedings of Conference on Piston Engines. USSR Academy of sciences, Moscow, pp. 185–191 (1956)
5. Ghojel, J.I.: Review of the development and applications of the wiebe function: a tribute to the contribution of ivan wiebe to engine research. Int. J. Engine Res. **11**(4), 297–312 (2010)
6. Woschni, G.: A Universally Applicable Equation for the Instantaneous Heat Transfer Coefficient in the Internal Combustion Engine. Technical report, SAE Technical paper (1967)
7. Finol, C.A., Robinson, K.: Thermal modelling of modern engines: a review of empirical correlations to estimate the in-cylinder heat transfer coefficient. Proc. Inst. Mech. Eng. Part D **220**(12), 1765–1781 (2006)
8. Heywood, J.B., et al.: Internal Combustion Engine Fundamentals. McGraw-Hill Book Company, New York (1988)
9. Heywood, J.B.: Pollutant formation and control in spark-ignition engines. In: Energy and Combustion Science, pp. 229–258. Elsevier, Amsterdam (1979)
10. Hiroyasu, H., Kadota, T.: Models for combustion and formation of nitric oxide and soot in direct injection diesel engines. SAE Trans. **85**, 513–526 (1976)
11. Amsden, A.A., Ramshaw, J.D., O'rourke, P.J., Dukowicz, J.K.: Kiva: A Computer Program for Two-and Three-Dimensional Fluid Flows with Chemical Reactions and Fuel Sprays. Technical report, Los Alamos National Lab., NM (USA) (1985)
12. Jiang, S., Nutter, D., Gullitti, A.: Implementation of Model-Based Calibration for a Gasoline Engine. Technical report, SAE technical paper (2012)
13. Mäkelä, M.: Experimental design and response surface methodology in energy applications: a tutorial review. Energy Convers. Manag. **151**, 630–640 (2017)
14. Bozza, F., De Bellis, V., Teodosio, L.: A numerical procedure for the calibration of a turbocharged spark-ignition variable valve actuation engine at part load. Int. J. Engine Res. **18**(8), 810–823 (2017)
15. Haghighatkhah, A., Banijamali, A., Pakanen, O.-P., Oivo, M., Kuvaja, P.: Automotive software engineering: a systematic mapping study. J. Syst. Softw. **128**, 25–55 (2017)
16. Lee, S., Jeon, J., Park, S.: Optimization of combustion chamber geometry and operating conditions for compression ignition engine fueled with pre-blended gasoline-diesel fuel. Energy Convers. Manag. **126**, 638–648 (2016)
17. Yongfan, L., Shuai, Z., Jing, W.: Research on the optimization design of motorcycle engine based on doe methodology. Procedia Eng. **174**, 740–747 (2017)
18. Kleijnen, J.P.C.: Design and analysis of simulation experiments. In: International Workshop on Simulation, pp. 3–22. Springer, Berlin (2015)
19. Morrison, P.: Driving Efficiency in Design for Rare Events Using Metamodeling and Optimization. PhD thesis, Boston University (2015)

20. Alsyouf, I., Al-Alami, A., Saidam, A.: Implementing product design development methodology for assessing and improving the performance of products. IJIDeM **9**(3), 225–234 (2015)
21. Lanzotti, A., Carbone, F., Grazioso, S., Renno, F., Staiano, M.: A new interactive design approach for concept selection based on expert opinion. IJIDeM **12**(4), 1189–1199 (2018)
22. Fischer, X., Coutellier, D.: Research in Interactive Design: Proceedings of Virtual Concept 2005. Springer, New York (2006)
23. Demuynck, J., Chana, K., De Paepe, M., Verhelst, S.: Evaluation of a Flow-Field-Based Heat Transfer Model for Premixed Spark-Ignition Engines on Hydrogen. Technical report, SAE technical paper (2013)
24. Carvalho, R.N., Machado, G.B., Colaço, M.J.: Prediction of internal combustion engines performance related to fuel properties using radial basis functions. Blucher Eng. Proc. **1**(2), 213–223 (2014)
25. Najafi, G., Ghobadian, B., Yusaf, T., Ardebili, S.M.S., Mamat, R.: Optimization of performance and exhaust emission parameters of a si (spark ignition) engine with gasoline-ethanol blended fuels using response surface methodology. Energy **90**, 1815–1829 (2015)
26. Chen, L., Zhang, Z., Gong, W., Liang, Z.: Quantifying the effects of fuel compositions on GDI-derived particle emissions using the optimal mixture design of experiments. Fuel **154**, 252–260 (2015)
27. Broekaert, S., Demuynck, J., De Cuyper, T., De Paepe, M., Verhelst, S.: Heat transfer in premixed spark ignition engines. Part I: Identification of the factors influencing heat transfer. Energy **116**, 380–391 (2016)
28. Yusri, I.M., Mamat, R., Azmi, W.H., Omar, A.I., Obed, M.A., Shaiful, A.I.M.: Application of response surface methodology in optimization of performance and exhaust emissions of secondary butyl alcohol-gasoline blends in SI engine. Energy Convers. Manag. **133**, 178–195 (2017)
29. Park, S., Song, S.: Model-based multi-objective pareto optimization of the bsfc and nox emission of a dual-fuel engine using a variable valve strategy. J. Nat. Gas Sci. Eng. **39**, 161–172 (2017)
30. Awad, O.I., Mamat, R., Ali, O.M., Azmi, W.H., Kadirgama, K., Yusri, I.M., Leman, A.M., Yusaf, T.: Response surface methodology (RSM) based multi-objective optimization of fusel oil-gasoline blends at different water content in SI engine. Energy Convers. Manag. **150**, 222–241 (2017)
31. Kleijnen, J.P.C.: Simulation experiments in practice: statistical design and regression analysis. J. Simul. **2**(1), 19–27 (2008)
32. Balki, M.K., Sayin, C., Canakci, M.: The effect of different alcohol fuels on the performance, emission and combustion characteristics of a gasoline engine. Fuel **115**, 901–906 (2014)
33. Masum, B.M., Masjuki, H.H., Kalam, M.A., Palash, S.M., Habibullah, M.: Effect of alcohol-gasoline blends optimization on fuel properties, performance and emissions of a SI engine. J. Clean. Prod. **86**, 230–237 (2015)
34. Elfasakhany, A.: Experimental study on emissions and performance of an internal combustion engine fueled with gasoline and gasoline/n-butanol blends. Energy Convers. Manag. **88**, 277–283 (2014)
35. Phuangwongtrakul, S., Wechsatol, W., Sethaput, T., Suktang, K., Wongwises, S.: Experimental study on sparking ignition engine performance for optimal mixing ratio of ethanol–gasoline blended fuels. Appl. Therm. Eng. **100**, 869–879 (2016)
36. Grasreiner, S., Neumann, J., Wensing, M., Hasse, C.: Model-based virtual engine calibration with the help of phenomenological methods for spark-ignited engines. Appl. Therm. Eng. **121**, 190–199 (2017)
37. Shi, L., Ji, C., Wang, S., Cong, X., Teng, S., Wang, D.: Combustion and emissions characteristics of a SI engine fueled with gasoline-dme blends under different spark timings. Fuel **211**, 11–17 (2018)
38. Doğan, B., Erol, D., Yaman, H., Kodanli, E.: The effect of ethanol–gasoline blends on performance and exhaust emissions of a spark ignition engine through exergy analysis. Appl. Therm. Eng. **120**, 433–443 (2017)
39. Wang, S., Prucka, R., Zhu, Q., Prucka, M., Dourra, H.: A real-time model for spark ignition engine combustion phasing prediction. SAE Int. J. Eng. **9**(1), 1180–1190 (2016). https://doi.org/10.4271/2016-01-0819
40. Amaya, A.F.D., Torres, A.G.D., Maya, D.A.A.: First and second thermodynamic law analyses applied to spark ignition engines modelling and emissions prediction. IJIDeM **10**(4), 401–415 (2016)
41. Zareei, J., Kakaee, A.H.: Study and the effects of ignition timing on gasoline engine performance and emissions. Eur. Transp. Res. Rev. **5**(2), 109–116 (2013)
42. de Carvalho, R.N., Machado, G.B., Colaço, M.J.: Estimating gasoline performance in internal combustion engines with simulation metamodels. Fuel **193**, 230–240 (2017)
43. Yamin, J.A.A., Gupta, H.N., Bansal, B.B., Srivastava, O.N.: Effect of combustion duration on the performance and emission characteristics of a spark ignition engine using hydrogen as a fuel. Int. J. Hydrog. Energy **25**(6), 581–589 (2000)
44. Sayin, C.: The impact of varying spark timing at different octane numbers on the performance and emission characteristics in a gasoline engine. Fuel **97**, 856–861 (2012)
45. Binjuwair, S., Alkudsi, A.: The effects of varying spark timing on the performance and emission characteristics of a gasoline engine: a study on saudi arabian ron91 and ron95. Fuel **180**, 558–564 (2016)
46. Yücesu, H.S., Sozen, A., Topgül, T., Arcaklioğlu, E.: Comparative study of mathematical and experimental analysis of spark ignition engine performance used ethanol-gasoline blend fuel. Appl. Therm. Eng. **27**(2–3), 358–368 (2007)
47. Hrovat, D., Sun, J.: Models and control methodologies for IC engine idle speed control design. Control Eng. Pract. **5**(8), 1093–1100 (1997)
48. Ji, C., Wang, S.: Strategies for improving the idle performance of a spark-ignited gasoline engine. Int. J. Hydrog. Energy **37**(4), 3938–3944 (2012)
49. Hao, L., Chen, W., Li, L., Tan, J., Wang, X., Yin, H., Ding, Y., Ge, Y.: Modeling and predicting low-speed vehicle emissions as a function of driving kinematics. J. Environ. Sci. **55**, 109–117 (2017)
50. Berger, P.D., Maurer, R.E.: Experimental Design. Wadsworth/Thomson Learning, Belmont (2002)
51. Daniel, C.: Use of half-normal plots in interpreting factorial two-level experiments. Technometrics **1**(4), 311–341 (1959)
52. Lenth, R.V.: Quick and easy analysis of unreplicated factorials. Technometrics **31**(4), 469–473 (1989)
53. Bozdogan, H.: Model selection and Akaike's information criterion (AIC): The general theory and its analytical extensions. Psychometrika **52**(3), 345–370 (1987)
54. Zhu, X., Chen, F., Guo, X., Zhu, L.: Heteroscedasticity testing for regression models: a dimension reduction-based model adaptive approach. Comput. Stat. Data Anal. **103**, 263–283 (2016)